Olive oil industry by-products. Effects of a polyphenol-rich extract on the metabolome and response to inflammation in cultured intestinal cell

(Article begins on next page)

25 April 2024

OLIVE OIL INDUSTRY BY-PRODUCTS. EFFECTS OF A POLYPHENOL-RICH EXTRACT ON THE METABOLOME AND RESPONSE TO INFLAMMATION IN CULTURED INTESTINAL CELL

Mattia Di Nunzio[a1], Gianfranco Picone[a1], Federica Pasini[b], Maria Fiorenza Caboni[a,b], Andrea Gianotti[a,b], Alessandra Bordoni[a,b,*], Francesco Capozzi[a,b]

Affiliation

[a]Department of Agri-Food Sciences and Technologies (DISTAL), University of Bologna, Piazza Goidanich 60, 47521 Cesena, Italy

[b]Interdepartmental Centre for Industrial Agri-Food Research (CIRI), University of Bologna, Piazza Goidanich 60, 47521 Cesena, Italy

[1]Both authors contributed equally to this work

* Corresponding author

Alessandra Bordoni

Department of Agri-Food Sciences and Technologies (DISTAL), University of Bologna, Piazza Goidanich 60, 47521 Cesena, Italy

e-mail: alessandra.bordoni@unibo.it

Phone: +39 0547338955

Abbreviations: ABTS, 2,2'-azinobis 3-ethylbenzothiazoline-6-sulfonate; AFOA, aldehydic form of oleuropein aglycone; d6-DSS, 2,2-dimethyl-2-silapentane-d6-5-sulfonic; DAFOA, dialdehydic form of oleuropein aglycone; DMEM, Dulbecco's modified Eagle's medium; DOP, defatted olive pomace; DPBS, Dulbecco's phosphate-buffered saline; GAE, gallic acid equivalent; GLUT2, glucose transporter 2; IFNγ, interferon gamma; IL-10, interleukin 10; IL-12p70, interleukin 12p70; IL-1α, interleukin 1 alpha; IL-1β, interleukin 1 beta; IL-2, interleukin 2; IL-4, interleukin 4; IL-6, interleukin 6; IL-8, interleukin 8; LDH, lactate dehydrogenase; MTT, methylthiazolyldiphenyl-tetrazolium bromide; MUFA, mono unsaturated fatty acids; NADH, nicotinamide adenine dinucleotide; PC, principal component; PCA, principal component analysis; PRE, polyphenol-rich extract; PUFA, poly unsaturated fatty acids; SGLT1, sodium-glucose transporter 1; TAC, total antioxidant capacity; TB, Trypan Blue; TE, trolox equivalent; TNFα, tumor necrosis factor alpha; TPC, total phenol content

Abstract

Over the past years, researchers and food manufacturers have become increasingly interested in olive polyphenols due to the recognition of their biological properties and probable role in the prevention of various diseases such as inflammatory bowel disease. Olive pomace, one of the main by-products of olive oil production, is a potential low-cost, phenol-rich ingredient for the formulation of functional food. In this study, the aqueous extract of olive pomace was characterized and used to supplement human intestinal cell in culture (Caco-2). The effect on the cell metabolome and the anti-inflammatory potential were then evaluated. Modification in the metabolome induced by supplementation clearly evidenced a metabolic shift toward a "glucose saving/accumulation" strategy that could have a role in maintaining anorexigenic hormone secretion and could explain the reported appetite-suppressing effect of the administration of polyphenol-rich food. In both basal and inflamed condition, supplementation significantly reduced the secretion of the main pro-inflammatory cytokine, IL-8. Thus, our data confirm the therapeutic potential of polyphenols, and specifically of olive pomace in intestinal bowel diseases. Although intervention studies are needed to confirm the clinical significance of our findings, the herein reported results pave the road for exploitation of olive pomace in the formulation of new, value-added foods. In addition, the application of a foodomics approach allowed observing a not hypothesized modulation of glucose metabolism.

1. INTRODUCTION

Olive oil is one of the most representative food in the traditional Mediterranean diet and a key element associated with its health-protecting effects. Epidemiological studies indicate an inverse association between olive oil intake and the occurrence of different types of cancer, cardiovascular risk factors, age-related processes, chronic inflammatory disorders, and inflammatory bowel diseases (Buckland & Gonzalez, 2015; Cougnard-Grégoire et al., 2016; Guasch-Ferré et al., 2014; Psaltopoulou, Kosti, Haidopoulos, Dimopoulos, & Panagiotakos, 2011; Schwingshackl, Christoph, & Hoffmann, 2015). These health benefits are mainly attributed to the phenolic class, where oleuropein, tyrosol and their derivatives are the major constituents and make up around 90% of the total phenolic content of a virgin olive oil (Talhaoui et al., 2016). Olive oil production, an agro-industrial activity of vital economic significance for many Mediterranean countries, is associated with the generation up to 30 million tons of waste by-products per year (Chandra & Sathiavelu, 2009), olive pomace being one of the main by-products (Mirabella, Castellani, & Sala, 2014).

Although olive mill wastes represent an important environmental problem in the Mediterranean area since their high organic acid concentration turns them into phytotoxic materials, they still contain valuable nutritional resources (Roig, Cayuela, & Sánchez-Monedero, 2006). After milling, only 2% of the phenolic compounds in olives is transferred to the oil and as much as 98% is retained in the cake. In particular, olive pomace has a high concentration of minerals, sugars and polyphenols (Dermeche, Nadour, Larroche, Moulti-Mati, & Michaud, 2013), and its possible valorization as functional ingredient deserves attention and represents a challenge for the food industry (Aliakbarian, Casazza, & Perego, 2011).

In this work, the polyphenols retained in the defatted olive pomace (DOP) were water extracted and quantitative and qualitative characterized, and the polyphenol-rich extract (PRE) was then supplemented to a human intestinal cell line (Caco-2 cells). Caco-2 is a colonic tumor cell line which, when cultured, spontaneously exhibits enterocyte-like characteristics. Given the difficulties in maintaining long-lasting cultures of enterocytes, this cell line is a suitable *in vitro* model to carry out experiments trying to delineate the effect of exogenous compounds (Rodríguez-Juan et al., 2001). The effect of PRE supplementation on the cell metabolome was investigated. The metabolomic approach, based on high-resolution NMR spectroscopy, allows determining the cell perturbation induced on cells by different concentration of polyphenols from a holistic point of view (Nicholson, Lindon, & Holmes, 1999; Picone et al., 2013). Moreover, the anti-inflammatory effect of PRE was evaluated by measuring the secretion of different cytokines in basal condition and in cells exposed to a pro-inflammatory stimulus.

In vitro experiments represent the first step to evaluate the health effect of new functional ingredients. Although clinical studies are needed before drawing conclusions, results herein reported clearly evidenced the anti-inflammatory effect of PRE and pave the road to the exploitation of olive pomace waste as a functional ingredient.

2.   MATERIAL & METHODS

2.1.   *Chemicals*

Dulbecco's modified Eagle's medium (DMEM), penicillin, streptomycin, and Dulbecco's phosphate-buffered saline (DPBS) were purchased from Lonza (Basel, Switzerland). Trypan Blue (TB) was from Bio-Rad Laboratories (Hercules, CA, USA). All other chemicals and solvents were of the highest analytical grade from Sigma-Aldrich Co. (St. Louis, MO, USA).

2.2.   *Polyphenol water extraction from defatted olive pomace (DOP) powder*

DOP powder was gently provided by ISANATUR SPAIN S.L. (Puente La Reina, Spain). Specifically, the by-product of olive oil extraction was dried and defatted based on the patent WO2013030426 with further developments to increase the process sustainability. DOP nutritional composition was analysed by producer (Table 1). Two g of DOP powder were suspended in 100 ml of distilled water, vigorously vortexed with a magnetic stirrer for 10 minutes at room temperature and sonicated at the maximum intensity for 44 minutes at 40 °C (Annegowda, Anwar, Mordi, Ramanathan, & Mansor, 2010). The solution was then centrifuged at 4,500g for 5 minutes and the supernatant sterilely filtered on 0.22 μm acetate cellulose filters. Two independent extractions were pooled to avoid technical inter-variability and kept at -20 °C until further analysis.

2.3.   *Total antioxidant capacity (TAC) and total phenol content (TPC)*

TAC was determined in PRE by the 2,2'-azinobis 3-ethylbenzothiazoline-6-sulfonate (ABTS) method as described by Di Nunzio, Toselli, Verardo, Caboni, and Bordoni (2013) and expressed as mM of trolox equivalent (TE). TPC content in PRE was determined using Folin–Ciocalteu's method adapted to a 96-well plate assay (Di Nunzio et al., 2013), and expressed as mg gallic acid equivalent (GAE)/mL.

2.4. Polyphenol composition by RP-HPLC–DAD–MS

The polyphenol composition of the extract was determined using a liquid chromatography apparatus HP 1100 series from Agilent Technologies coupled to diode array and mass spectrometer detectors, as previously described by Gómez-Caravaca et al. (2013), with some modification. The sample was injected in a reverse phase column Poroshell 120 SB-C18 (3 x 100 mm, 2.7 µm) from Phenomenex, and the chromatogram was registered at 280 nm. The extracted compounds were identified by analysing UV and MS spectra and quantified by DAD detection. The quantification was performed by comparison to calibration curves of tyrosol, caffeic acid, oleuropein and rutin at 280 nm for the different class of phenols.

2.5. Caco-2 cell culture and supplementation

Caco-2 cells were seeded in 24-well and 96-well plates at 1×10^5 cells/well concentration (cytotoxicity and inflammation assays) or in 100 mm Petri dishes at 2.7×10^6 cells/well (NMR assay) and grown for 21 days. After complete differentiation, assessed by measuring the trans epithelial electric resistance of the cell monolayer using a commercial apparatus (Millicell ERS; Millipore Co., Bedford, MA), cells were supplemented for 24 h with 1 ml of serum-free DMEM containing different amount of PRE-polyphenols (10, 20, 50, 100, 200 and 500 µg/ml). To avoid interference due to the vehicle, some cells were supplemented with the same amount of water (control cells). To induce inflammation, in some experiments cells were exposed to interleukin 1 beta (IL-1β) at 10 ng/mL for 24 h. The inflammatory stimulus was concomitant to PRE supplementation.

2.6. Cytotoxicity

PRE cytotoxicity was evaluated in Caco-2 cells by different assays:
- The number of total and viable cells was determined by staining cell populations with TB as reported by Di Nunzio et al. (2013) with slight modifications. Cell viability was expressed as a percentage of the total cell number.
- Cell viability was assessed using AlamarBlue® Cell Viability Reagent (Life Technologies Ltd.; Paisley, UK) and the methylthiazolyldiphenyl-tetrazolium bromide (MTT) assay with slight modifications (Di Nunzio et al., 2013; Valli, Taccari, Di Nunzio, Danesi, & Bordoni, 2018). Cell viability was expressed as a percentage of the viability in control cells, assigned as 100%.

5

148   -   Lactate dehydrogenase (LDH) release was assessed determining its activity in the medium. The

149   rate of nicotinamide adenine dinucleotide (NADH) oxidation was followed

150   spectrophotometrically at 340 nm for 1 min (Di Nunzio, Valli, & Bordoni, 2016), and LDH

151   activity was calculated using the extinction coefficient of NADH, normalized for cell cell count

152   and expressed as mU/ml/10^6 cells.

153

2.7. HR ^{1}H-NMR

156   Cells were scraped off and the pellet washed with ice-cold DPBS. Cells were then lysed by

157   sonication and centrifuged at 21,000g for 10 min at 4 °C. Five hundred μl of supernatant were

158   centrifuged at 14,000rpm for 5 min and then added to 10 μl of a D2O solution of 100 mM 2,2-

159   dimethyl-2-silapentane-d6-5-sulfonic (d6-DSS) with a final concentration in the NMR tube of

160   9.0909 mM. ^{1}H-NMR spectra were recorded at 298 K on a Bruker US+ Avance III spectrometer

161   operating at 600 MHz, equipped with a BBI-z probe and a B-ACS 60 sampler for automation

162   (Bruker BioSpin, Karlsruhe, Germany). The HOD residual signal was suppressed by applying the

163   CPMGPR1D sequence with presaturation. Each spectrum was acquired using 32 K data points over

164   a 7183.908 Hz spectral width (12 ppm) and adding 256 transients. A recycle delay (D1) of 5 s and a

165   90° pulse (P1) of 11.190 μs were set up. Acquisition time (2.28 s) and recycle delay were adjusted

166   to be 5 times longer than the longitudinal relaxation time (T1) of the protons under investigation,

167   which has been considered to be not longer than 1.4. The data were Fourier transformed and phase

168   and baseline corrections were automatically performed using TopSpin version 3.0 (Bruker BioSpin,

169   Karlsruhe, Germany). Signals were identified by comparing their chemical shift and multiplicity

170   with Chenomx Profiler software data bank (ver. 8.1, Edmonton, Canada) and data in the literature

171   (Ghini et al., 2017; Picone et al., 2013).

2.8. Cytokines secretion

175   After 24 h supplementation, the level of the pro- and anti-inflammatory cytokines interferon gamma

176   (IFNγ), interleukin 1 alpha (IL-1α), IL-1β, interleukin 2 (IL-2), interleukin 4 (IL-4), interleukin 6

177   (IL-6), interleukin (IL-8), interleukin 10 (IL-10), interleukin 12 p70 (IL-12p70), and tumor necrosis

178   factor alpha (TNFα) was estimated in the cell media by the multiplex sandwich ELISA Ciraplex

179   (Aushon; Billerica, USA) following the manufacturer's instructions. 96-well plates pre-spotted with

180   protein-specific antibodies were used and luminescent signals were detected by Cirascan™ Imaging

181   System. Results were expressed as pg/mL medium. The level of the pro-inflammatory IL-8 was

6

estimated in cell media also by AlphaLISA kits (IL-8 Immunoassay Research Kits; Perkin Elmer Inc., Waltham, MA, USA) following the manufacturer's instructions (Antognoni et al., 2017; Valli et al., 2016). 96-microwell plates (96 1/2 AreaPlate from Perkin Elmer) were used and read using an EnSpire™ plate reader (Perkin Elmer). Results were expressed as pg/mL medium.

2.9.   Statistical analysis

Compositional, cytotoxicity and inflammation data are mean ± standard deviation (SD). Statistical differences were determined by the one-way analysis of variance (ANOVA) followed by Dunnett's test considering $p < 0.05$ as significant. NMR spectra processing and statistical analyses were performed using R computational language (ver. 3.4.3) and MATLAB (ver R2008b, MathWorks Inc.). Each ^{1}H-NMR spectrum was processed by means of scripts developed in-house. ANOVA followed by Tukey HSD multiple comparison was performed on the integral of each bin. The outcomes of ANOVA ($p < 0.05$ as significant) pointed out metabolites affected in a positive or negative way (Picone et al., 2018).

3.   RESULTS

3.1.   PRE characterization

TAC and TPC of PRE are reported in Table 2. PRE phenolic profile and quantification are given in Fig. 1. As shown, 1-β-D-glucopyranosyl acyclodihydroelenolic acid/Hydroxytyrosol and β-hydroxyverbascoside were the main phenols in PRE.

3.2.   Cell count and viability

In Fig. 2, cell count and cell viability evaluated by TB (A), and by MTT assay, Alamar Blue, and LDH release (B) are reported. No modification in cell number, viability (TB and Alamar Blue) and LDH leakage was evidenced up to PRE concentration corresponding to 200 µg of polyphenols/mL. At the highest PRE concentration, a significant increase of cell number and viability, and a reduction of LDH release were observed. The MTT assay evidenced an enhanced cell viability also at PRE- concentrations corresponding to 100 and 200 µg of polyphenols/mL.

3.3.   Effect on the metabolome

7

To investigate the perturbation induced by supplementation on Caco-2 metabolome, PRE concentrations corresponding to 50, 200 and 500 μg polyphenols/mL were used. These concentrations were selected on the basis of cytotoxicity results, 50 μg/mL representing the highest concentration inducing no variation in cell viability, while 200 and 500 μg/mL were the two highest concentrations causing an increase of cell viability. Before statistics, each ^{1}H-NMR spectrum was processed by means of scripts developed in-house in R language. Chemical shift referencing was performed by setting the DSS signal to 0.00 ppm. Moreover, the alignment of the spectra was improved, where possible, using the *i*Coshift tool (Savorani, Tomasi, & Engelsen, 2010) available at http:// www.models.life.ku.dk/algorithms/. The following spectral regions were removed prior to data analysis: the regions including only noise (the spectrum edges between 11.00 and 9.00 ppm and between 0.5 and -1.00 ppm), the NMR signal which is strongly affected by the residual solvent peak (water, between 4.00 and 5.00 ppm). After the Fourier transformation and prior to multivariate analysis, data underwent to a pre statistical improvement: spectra were first normalized to the unit area (Craig, Cloarec, Holmes, Nicholson, & Lindon, 2006) and then a points reduction by the "spectral binning" (Gartland, Beddell, Lindon, & Nicholson, 1991). The first operation is aimed at removing possible dilution effects. The second one avoids the effect of peaks misalignments among different spectra due to variations in chemical shift of signals belonging to some titratable acids. The binning operation is performed by subdividing the spectra into 720 bins, each integrating 60 data points (0.0109 ppm each). Principal component analysis (PCA) was performed on 720 bins. A representative ^{1}H spectra of control and supplemented cell are shown in Fig. 3; to better appreciate small signals, spectra were split into two parts (A and B) and then magnified. To evaluate the effect of PRE on the cell metabolome and the variation within samples, a preliminary PCA was performed on the binned database (data not shown). The main function of PCA is to explain the highest portion of variance of the original data (Laghi, Picone, & Capozzi, 2014) and at the same time to reduce the number of variables of the dataset to two or three principal components. These new components correspond to a linear combination of the original ones and they are represented as a score plot where each principal component (PC) accounts for as much variance in the data as possible. PC1 vs PC2 account for 90% of the total variance and it is mainly located along PC1 (78%). The high variance explained by PC1 is because of the effect of PRE on cells' metabolome which changes deeply from 50 μg/mL to 500 μg/mL. A second PCA was run considering only bins with a loading value greater than the standard deviation of the principal component loading for PC1 and PC2. Results are shown in the score plots of Fig. 4A. To gain insight into the observed spectral clustering, the PCA loadings were inspected and the result plotted in Fig. 4B. The increasing doses

8

of PRE exerted metabolic changes along PC1, resulting in positive values of this principal component at low doses, whilst at higher concentration of PRE the metabolic pathways switch to a different condition, giving rise to PC1 negative values, indicating a drastic change in the metabolic pathways. To confirm that bins in the loading barplot were significantly different, ANOVA followed by Tukey HSD multiple comparison test was performed on the integral of each compound (Table 3).

3.4.   PRE anti-inflammatory activity

To evaluate PRE anti-inflammatory effect, cells were supplemented with the same concentrations used to assess the impact on metabolome. Cytokine secretion in the medium was evaluated by ELISA Ciraplex assay in basal condition and in cells exposed to an inflammatory stimulus (IL-1β), and it is reported in Table 4.

In basal condition, only IL-8 was detectable in the medium of control cells. Supplementation with PRE caused a significant decrease of the pro-inflammatory IL-8, while IL-1α slightly increased at the highest PRE concentration. In inflamed condition, an increased secretion of all cytokines was evident in control cells. Particularly, IL-8 concentration in the medium was 8 times higher than in basal condition. Co-administration of PRE phenols significantly reduced IL-8 secretion in a dose-related manner. Notably, in inflamed condition, IL-8 concentration in cells supplemented with 500 μg/mL phenols was lower than in control cells in basal condition. Supplementation with the highest PRE concentration also caused an increase in IL-1α and IL-10 secretion compared to control cells. After 24 h, IL-1β concentration was lower than the supplemented concentration confirming its very short half-life in a biological system (Lopez-Castejon & Brough, 2011). IL-8 secretion was also determined using the AlphaLISA kit assay. As reported in Fig. 5, results obtained confirmed the previous ones.

4.   DISCUSSION

A relevant challenge for scientists and food industries is to turn food processing by-products and wastes into new ingredients exploiting the favorable properties that this low-price, yet very nutritious, commodities have (Moure et al., 2001). In this study, we focused on the possible exploitation of olive oil by-products evaluating the effect of PRE of olive pomace in cultured intestinal cells. The first step was to evaluate and characterize the PRE, and data obtained were consistent with previous results on olive pomace (De Marco, Savarese, Paduano, & Sacchi, 2007;

Ghanbari, Anwar, Alkharfy, Gilani, & Saari, 2012; Malapert, Reboul, Loonis, Dangles, & Tomao, 2018).

Although extracts containing a high concentration of phenols can be considered high valued products, knowledge of their cellular effects is required to evaluate their potential as a value-added functional ingredient. To this aim, Caco-2 cells were supplemented with different concentrations of PRE providing a different amount of phenolic compounds. The possible cytotoxicity of PRE was assessed, and no cytotoxic effects were observed. On the contrary, the highest PRE concentration (500 μg polyphenols/mL) reduced LDH leakage and increased cell viability. The MTT assay revealed a significant increase of viability also in cells supplemented with lower PRE concentrations (100 and 200 μg polyphenols/mL). It could be due not only to the high sensitivity of the assay (Di Nunzio et al., 2017), but also to an increased mitochondrial activity. In fact, the measurement of cell viability using the MTT assay correlates with the mitochondrial metabolic capacity (Danesi et al., 2011). de Oliveira et al. (2016) already showed that resveratrol positively modulates mitochondrial activity. This effect could be ascribed to the incorporation of phenolic compounds that induces a deformation of the membrane surface toward a negative membrane curvature (Lopez et al., 2014) modulating pathways that define mitochondrial biogenesis, membrane potential, electron transport chain and adenosine triphosphate synthesis, and intra-mitochondrial oxidative status (Sandoval-Acuna, Ferreira, & Speisky, 2014). Although previous studies have identified specific metabolic properties of olive phenols (Rescifina, Chiacchio, Iannazzo, Piperno, & Romeo, 2010), their overall impact on the cell metabolome is still unknown. This issue was addressed in this study investigating the effects of PRE supplementation on the entire metabolome by ^{1}HNMR techniques combined with pattern recognition (Picone et al., 2011). Using an untargeted approach, we evidenced that olive polyphenols supplementation causes a huge dose-related perturbation of Caco-2 cells metabolome. In particular, PRE supplementation modified glucose homeostasis and metabolism. The increased intracellular concentration of glucose (both in phosphorylated and unphosphorylated form) was related to a reduced catabolization, as confirmed by the decreased concentration of pyruvate and lactate. *In vitro* and *in vivo* studies already reported that various polyphenols and their derivatives may impair the glycolytic pathway through the inhibition of phosphofructokinase, glyceraldehyde 3-phosphate dehydrogenase and pyruvate kinase activity (Ishii et al., 2008; Li et al., 2016; Rodacka, Strumillo, Serafin, & Puchala, 2015). In addition, we could speculate that modification in glucose transport also occurred. Glucose is absorbed by intestinal cells mainly via the sodium-glucose transporter 1 (SGLT1), and it is then released in the blood stream via glucose transporter 2 (GLUT2) (Röder et al., 2014). Glucose transporters are inhibited by different polyphenols (Castro-Acosta, Lenihan-Geels, Corpe, & Hall,

10

2016; Schulze et al., 2014), and inhibition of GLUT2 is reported to be stronger than SGLT1 (Farrell, Ellam, Forrelli, & Williamson, 2013; Manzano & Williamson, 2010). The increased glucose intracellular concentration could be also due to an increased gluconeogenesis from alanine, which significantly decreased in cells supplemented with the highest PRE concentration. A gluconeogenetic activity in Caco-2 cells has been already reported (Pan et al., 2003) and intestinal glucose *de-novo* synthesis has a role in the regulation of satiety and food intake (Mithieux et al., 2005). The modification of the concentration of the two ketogenetic aminoacids, leucine and isoleucine, and of myo-inositol and taurine, which are both linked to glucose metabolism, are also suggestive of a metabolic shift toward a "glucose saving/accumulation" strategy. The gastrointestinal tract releases hormones with important physiological roles in regulating plasma glucose levels, gut motility and satiety. Gut hormones cholecystokinin, glucagon-like peptide and peptide tyrosine-tyrosine have been shown to be the primary satiety signals, and their secretion is regulated by nutrient intake (Wren & Bloom, 2007) and by the concentration of intestinal glucose (Sun et al., 2017). Caco-2 cells secrete anorexigenic gut hormones, and secretion is induced by exposure to epigallocatechin-3-gallate, chlorogenic acid and ferulic acid (Song, Aihara, Hashimoto, Kanazawa, & Mizuno, 2015). The observed glucose accumulation after exposure to PRE could have a role in maintaining anorexigenic hormone secretion, and could explain the reported appetite-suppressing effect of the administration of polyphenol-rich food (Molan, Lila, & Mawson, 2008). Further studies are needed both *in vitro* and *in vivo* to verify this hypothesis and to understand its functional and clinical significance.

In basal condition, supplementation with the highest concentration of PRE-phenols significantly reduced IL-8 secretion; in inflammatory condition, the anti-inflammatory effect of PRE was dose-related. The major anti-inflammatory components in olives are tyrosol, hydroxytyrosol, oleuropein, verbascoside and their derivatives (Rigacci & Stefani, 2016). In particular, hydroxytyrosol is considered the major anti-inflammatory compound in aqueous olive extracts (Richard et al., 2011). In agreement, hydroxytyrosol and verbascoside were the main phenols in the PRE extract, and their rapid uptake by intestinal cells has been demonstrated in Caco-2 cells (Cardinali, Linsalata, Lattanzio, & Ferruzzi, 2011). Overall, our finding confirms the therapeutic potential of polyphenols in inflammatory bowel diseases (Rahman et al., 2018; Salaritabar et al., 2017).

The exploitation of by-products to formulate new food with added nutritional value is an innovative and sustainable strategy that meets current and future expectations of consumers about environmental impact, ethical issues, human health, and safety, maximizing the net benefit to society. To do it, by-products must be characterized and their effect in cells should be investigated in depth as a preparatory approach to human intervention trials. In this study, the anti-inflammatory

11

effect of an extract obtained from olive pomace has been clearly evidenced in cultured intestinal cells. A concomitant, not hypothesized modulation of glucose metabolism was observed, highlighting that NMR metabolomics is fundamental for studying the biological effect of bioactive compounds, particularly when they have a broad spectrum of mechanisms of action. Although Caco-2 cells are often used to investigate the anti-inflammatory effects of food components (Antognoni et al., 2017: Romier-Crouzet et al., 2009), the Authors are aware that results obtained *in vitro* must be confirmed *in vivo*. Anyway, the present research confirm that the foodomics approach has a great potentiality in the assessment of the nutraceutical properties of bioactive compounds (Capozzi & Bordoni, 2013; Catalan, Barrubes, Valls, Sola, & Rubio, 2017; Ghini et al., 2017; Marcolini et al., 2015).

Funding

Author contributions

M.D.N. performed the experiments on cell culture and wrote the manuscript; G.P. carried out NMR and multivariate statistical analysis; F.P. performed HPLC analyses; A.B., M.F.C., F.C. and A.G. designed and supervised the study. All Authors critically contributed to the manuscript writing.

Conflicts of interest

The authors declare no conflict of interest. The funding sponsors had no role in the design of the study; in the collection, analysis, or interpretation of data; in the writing of the manuscript, and in the decision to publish the results.

REFERENCES

Aliakbarian, B., Casazza, A. A., & Perego, P. (2011). Valorization of olive oil solid waste using high pressure–high temperature reactor. *Food chemistry, 128*(3), 704-710.

Annegowda, H. V., Anwar, L. N., Mordi, M. N., Ramanathan, S., & Mansor, S. M. (2010). Influence of sonication on the phenolic content and antioxidant activity of Terminalia catappa L. leaves. *Pharmacognosy Research, 2*(6), 368-373. doi: 10.4103/0974-8490.75457

Antognoni, F., Mandrioli, R., Bordoni, A., Di Nunzio, M., Viadel, B., Gallego, E., Villalba, M. P., Tomás-Cobos, L., Taneyo Saa, D. L., & Gianotti, A. (2017). Integrated Evaluation of the Potential Health Benefits of Einkorn-Based Breads. *Nutrients, 9*(11), 1232.

Antoshechkin, A. G. (2001). On intracellular formation of ethanol and its possible role in energy metabolism. *Alcohol and Alcoholism, 36*(6), 608-608.

Buckland, G., & Gonzalez, C. A. (2015). The role of olive oil in disease prevention: a focus on the recent epidemiological evidence from cohort studies and dietary intervention trials. *British journal of nutrition, 113*(S2), S94-S101.

Capozzi, F., & Bordoni, A. (2013). Foodomics: a new comprehensive approach to food and nutrition. *Genes & nutrition, 8*(1), 1. doi: https://doi.org/10.1007/s12263-012-0310-x

Cardinali, A., Linsalata, V., Lattanzio, V., & Ferruzzi, M. G. (2011). Verbascosides from olive mill waste water: Assessment of their bioaccessibility and intestinal uptake using an in estion/Caco-2 model system. *Journal of food science, 76*(2).

Castro-Acosta, M. L., Lenihan-Geels, G. N., Corpe, C. P., & Hall, W. L. (2016). Berries and anthocyanins: promising functional food ingredients with postprandial glycaemia-lowering effects. *Proceedings of the Nutrition Society, 75*(3), 342-355.

Catalan, U., Barrubes, L., Valls, R. M., Sola, R., & Rubio, L. (2017). In vitro Metabolomic Approaches to Investigating the Potential Biological Effects of Phenolic Compounds: An Update. *Genomics, proteomics & bioinformatics, 15*(4), 236-245.

Chandra, M., & Sathiavelu, S. (2009). Waste management in the olive oil industry in the Mediterranean region by composting. *Clean Technologies and Environmental Policy, 11*(3), 293-298.

Cougnard-Grégoire, A., Merle, B. M., Korobelnik, J.-F., Rougier, M.-B., Delyfer, M.-N., Le Goff, M., Samieri, C., Dartigues, J.-F., & Delcourt, C. (2016). Olive oil consumption and age-related macular degeneration: the ALIENOR Study. *PLoS ONE, 11*(7), e0160240.

Craig, A., Cloarec, O., Holmes, E., Nicholson, J. K., & Lindon, J. C. (2006). Scaling and normalization effects in NMR spectroscopic metabonomic data sets. *Analytical chemistry, 78*(7), 2262-2267.

Danesi, F., Ferioli, F., Caboni, M. F., Boschetti, E., Di Nunzio, M., Verardo, V., Valli, V., Astolfi, A., Pession, A., & Bordoni, A. (2011). Phytosterol supplementation reduces metabolic activity and slows cell growth in cultured rat cardiomyocytes. *British journal of nutrition, 106*(4), 540-548.

De Marco, E., Savarese, M., Paduano, A., & Sacchi, R. (2007). Characterization and fractionation of phenolic compounds extracted from olive oil mill wastewaters. *Food chemistry, 104*(2), 858-867.

de Oliveira, M. R., Nabavi, S. F., Manayi, A., Daglia, M., Hajheydari, Z., & Nabavi, S. M. (2016). Resveratrol and the mitochondria: from triggering the intrinsic apoptotic pathway to inducing mitochondrial biogenesis, a mechanistic view. *Biochimica et Biophysica Acta (BBA)-General Subjects, 1860*(4), 727-745.

Dermeche, S., Nadour, M., Larroche, C., Moulti-Mati, F., & Michaud, P. (2013). Olive mill wastes: Biochemical characterizations and valorization strategies. *Process Biochemistry, 48*(10), 1532-1552. doi: https://doi.org/10.1016/j.procbio.2013.07.010

Di Nunzio, M., Toselli, M., Verardo, V., Caboni, M. F., & Bordoni, A. (2013). Counteraction of oxidative damage by pomegranate juice: influence of the cultivar. *Journal of the Science of Food and Agriculture, 93*(14), 3565-3573.

Di Nunzio, M., Valli, V., & Bordoni, A. (2016). PUFA and oxidative stress. Differential modulation of the cell response by DHA. *International journal of food sciences and nutrition, 67*(7), 834-843.

Di Nunzio, M., Valli, V., Tomás-Cobos, L., Tomás-Chisbert, T., Murgui-Bosch, L., Danesi, F., & Bordoni, A. (2017). Is cytotoxicity a determinant of the different in vitro and in vivo effects of bioactives? *BMC complementary and alternative medicine, 17*(1), 453.

Farrell, T. L., Ellam, S. L., Forrelli, T., & Williamson, G. (2013). Attenuation of glucose transport across Caco-2 cell monolayers by a polyphenol-rich herbal extract: Interactions with SGLT1 and GLUT2 transporters. *Biofactors, 39*(4), 448-456.

Gartland, K., Beddell, C., Lindon, J., & Nicholson, J. (1991). Application of pattern recognition methods to the analysis and classification of toxicological data derived from proton nuclear magnetic resonance spectroscopy of urine. *Molecular Pharmacology, 39*(5), 629-642.

Ghanbari, R., Anwar, F., Alkharfy, K. M., Gilani, A.-H., & Saari, N. (2012). Valuable nutrients and functional bioactives in different parts of olive (Olea europaea L.)—a review. *International journal of molecular sciences, 13*(3), 3291-3340.

Ghini, V., Di Nunzio, M., Tenori, L., Valli, V., Danesi, F., Capozzi, F., Luchinat, C., & Bordoni, A. (2017). Evidence of a DHA signature in the lipidome and metabolome of human hepatocytes. *International journal of molecular sciences, 18*(2), 359.

Gómez-Caravaca, A. M., Verardo, V., Toselli, M., Segura-Carretero, A., Fernández-Gutiérrez, A., & Caboni, M. F. (2013). Determination of the major phenolic compounds in pomegranate juices by HPLC–DAD–ESI-MS. *Journal of agricultural and food chemistry, 61*(22), 5328-5337.

Guasch-Ferré, M., Hu, F. B., Martínez-González, M. A., Fitó, M., Bulló, M., Estruch, R., Ros, E., Corella, D., Recondo, J., & Gómez-Gracia, E. (2014). Olive oil intake and risk of cardiovascular disease and mortality in the PREDIMED Study. *BMC medicine, 12*(1), 78.

Ishii, T., Mori, T., Tanaka, T., Mizuno, D., Yamaji, R., Kumazawa, S., Nakayama, T., & Akagawa, M. (2008). Covalent modification of proteins by green tea polyphenol (−)-epigallocatechin-3-gallate through autoxidation. *Free Radical Biology and Medicine, 45*(10), 1384-1394. doi: https://doi.org/10.1016/j.freeradbiomed.2008.07.023

Laghi, L., Picone, G., & Capozzi, F. (2014). Nuclear magnetic resonance for foodomics beyond food analysis. *TrAC Trends in Analytical Chemistry, 59*, 93-102.

Li, S., Wu, L., Feng, J., Li, J., Liu, T., Zhang, R., Xu, S., Cheng, K., Zhou, Y., & Zhou, S. (2016). In vitro and in vivo study of epigallocatechin-3-gallate-induced apoptosis in aerobic glycolytic hepatocellular carcinoma cells involving inhibition of phosphofructokinase activity. *Scientific reports, 6*, 28479.

Lopez-Castejon, G., & Brough, D. (2011). Understanding the mechanism of IL-1β secretion. *Cytokine & growth factor reviews, 22*(4), 189-195.

Lopez, S., Bermudez, B., Montserrat-de la Paz, S., Jaramillo, S., Varela, L. M., Ortega-Gomez, A., Abia, R., & Muriana, F. J. (2014). Membrane composition and dynamics: a target of bioactive virgin olive oil constituents. *Biochimica et Biophysica Acta (BBA)-Biomembranes, 1838*(6), 1638-1656.

Malapert, A., Reboul, E., Loonis, M., Dangles, O., & Tomao, V. (2018). Direct and Rapid Profiling of Biophenols in Olive Pomace by UHPLC-DAD-MS. *Food Analytical Methods, 11*(4), 1001-1010.

Manzano, S., & Williamson, G. (2010). Polyphenols and phenolic acids from strawberry and apple decrease glucose uptake and transport by human intestinal Caco-2 cells. *Molecular nutrition & food research, 54*(12), 1773-1780.

Marcolini, E., Babini, E., Bordoni, A., Di Nunzio, M., Laghi, L., Maczó, A., Picone, G., Szerdahelyi, E., Valli, V., & Capozzi, F. (2015). Bioaccessibility of the bioactive peptide carnosine during in vitro digestion of cured beef meat. *Journal of agricultural and food chemistry, 63*(20), 4973-4978.

Mirabella, N., Castellani, V., & Sala, S. (2014). Current options for the valorization of food manufacturing waste: a review. *Journal of Cleaner Production, 65*, 28-41.

Mithieux, G., Misery, P., Magnan, C., Pillot, B., Gautier-Stein, A., Bernard, C., Rajas, F., & Zitoun, C. (2005). Portal sensing of intestinal gluconeogenesis is a mechanistic link in the diminution of food intake induced by diet protein. *Cell metabolism, 2*(5), 321-329.

Molan, A., Lila, M., & Mawson, J. (2008). Satiety in rats following blueberry extract consumption induced by appetite-suppressing mechanisms unrelated to in vitro or in vivo antioxidant capacity. *Food chemistry, 107*(3), 1039-1044.

Moure, A., Cruz, J. M., Franco, D., Domínguez, J. M., Sineiro, J., Domínguez, H., Núñez, M. a. J., & Parajó, J. C. (2001). Natural antioxidants from residual sources. *Food chemistry, 72*(2), 145-171.

Nicholson, J. K., Lindon, J. C., & Holmes, E. (1999). 'Metabonomics': understanding the metabolic responses of living systems to pathophysiological stimuli via multivariate statistical analysis of biological NMR spectroscopic data. *Xenobiotica, 29*(11), 1181-1189.

Nikolaenko, V. (2001). Maintenance of Homeostasis of Endogenous Ethanol as a Method for the Therapy of Alcoholism. *Bulletin of experimental biology and medicine, 131*(3), 231-233.

Pan, G.-Y., Huang, Z.-J., Wang, G.-J., Fawcett, J. P., Liu, X.-D., Zhao, X.-C., Sun, J.-G., & Xie, Y.-Y. (2003). The antihyperglycaemic activity of berberine arises from a decrease of glucose absorption. *Planta Medica, 69*(07), 632-636.

Picone, G., Laghi, L., Gardini, F., Lanciotti, R., Siroli, L., & Capozzi, F. (2013). Evaluation of the effect of carvacrol on the Escherichia coli 555 metabolome by using 1H-NMR spectroscopy. *Food chemistry, 141*(4), 4367-4374.

Picone, G., Mezzetti, B., Babini, E., Capocasa, F., Placucci, G., & Capozzi, F. (2011). Unsupervised principal component analysis of NMR metabolic profiles for the assessment of substantial equivalence of transgenic grapes (Vitis vinifera). *Journal of agricultural and food chemistry, 59*(17), 9271-9279.

Picone, G., Zappaterra, M., Luise, D., Trimigno, A., Capozzi, F., Motta, V., Davoli, R., Costa, L. N., Bosi, P., & Trevisi, P. (2018). Metabolomics characterization of colostrum in three sow breeds and its influences on piglets' survival and litter growth rates. *Journal of animal science and biotechnology, 9*(1), 23.

Psaltopoulou, T., Kosti, R. I., Haidopoulos, D., Dimopoulos, M., & Panagiotakos, D. B. (2011). Olive oil intake is inversely related to cancer prevalence: a systematic review and a meta-analysis of 13800 patients and 23340 controls in 19 observational studies. *Lipids in health and disease, 10*(1), 127.

Rahman, S. U., Li, Y., Huang, Y., Zhu, L., Feng, S., Wu, J., & Wang, X. (2018). Treatment of inflammatory bowel disease via green tea polyphenols: possible application and protective approaches. *Inflammopharmacology*, 1-12.

Rescifina, A., Chiacchio, U., Iannazzo, D., Piperno, A., & Romeo, G. (2010). β-cyclodextrin and caffeine complexes with natural polyphenols from olive and olive oils: NMR, thermodynamic, and molecular modeling studies. *Journal of agricultural and food chemistry, 58*(22), 11876-11882.

Richard, N., Arnold, S., Hoeller, U., Kilpert, C., Wertz, K., & Schwager, J. (2011). Hydroxytyrosol is the major anti-inflammatory compound in aqueous olive extracts and impairs cytokine and chemokine production in macrophages. *Planta Medica-Natural Products and MedicinalPlant Research, 77*(17), 1890.

Rigacci, S., & Stefani, M. (2016). Nutraceutical properties of olive oil polyphenols. An itinerary from cultured cells through animal models to humans. *International journal of molecular sciences, 17*(6), 843.

Righi, V., Di Nunzio, M., Danesi, F., Schenetti, L., Mucci, A., Boschetti, E., Biagi, P., Bonora, S., Tugnoli, V., & Bordoni, A. (2011). EPA or DHA supplementation increases triacylglycerol, but not phospholipid, levels in isolated rat cardiomyocytes. *Lipids, 46*(7), 627-636.

Rodacka, A., Strumillo, J., Serafin, E., & Puchala, M. (2015). Analysis of potential binding sites of 3, 5, 4′-trihydroxystilbene (resveratrol) and trans-3, 3′, 5, 5′-tetrahydroxy-4′-methoxystilbene (THMS) to the GAPDH molecule using a computational ligand-docking method: structural and functional changes in GAPDH induced by the examined polyphenols. *The Journal of Physical Chemistry B, 119*(30), 9592-9600.

Röder, P. V., Geillinger, K. E., Zietek, T. S., Thorens, B., Koepsell, H., & Daniel, H. (2014). The role of SGLT1 and GLUT2 in intestinal glucose transport and sensing. *PLoS ONE, 9*(2), e89977.

Rodríguez-Juan, C., Perez-Blas, M., Valeri, A., Aguilera, N., Arnaiz-Villena, A., Pacheco-Castro, A., & Martín-Villa, J. (2001). Cell surface phenotype and cytokine secretion in Caco-2 cell cultures: increased RANTES production and IL-2 transcription upon stimulation with IL-1β. *Tissue and Cell, 33*(6), 570-579.

Roig, A., Cayuela, M., & Sánchez-Monedero, M. (2006). An overview on olive mill wastes and their valorisation methods. *Waste Management, 26*(9), 960-969.

Romier-Crouzet B, Van De Walle, J., During, A., Joly, A., Rousseau, C., Henry, O., Larondelle, Y., Schneider YJ. (2009) Inhibition of inflammatory mediators by polyphenolic plant extracts in human intestinal Caco-2 cells. *Food Toxicology, 47*(6) 1221-1230.

Salaritabar, A., Darvishi, B., Hadjiakhoondi, F., Manayi, A., Sureda, A., Nabavi, S. F., Fitzpatrick, L. R., Nabavi, S. M., & Bishayee, A. (2017). Therapeutic potential of flavonoids in inflammatory bowel disease: A comprehensive review. *World journal of gastroenterology, 23*(28), 5097.

Sandoval-Acuna, C., Ferreira, J., & Speisky, H. (2014). Polyphenols and mitochondria: an update on their increasingly emerging ROS-scavenging independent actions. *Archives of biochemistry and biophysics, 559*, 75-90.

Savorani, F., Tomasi, G., & Engelsen, S. B. (2010). icoshift: A versatile tool for the rapid alignment of 1D NMR spectra. *Journal of Magnetic Resonance, 202*(2), 190-202.

Schulze, C., Bangert, A., Kottra, G., Geillinger, K. E., Schwanck, B., Vollert, H., Blaschek, W., & Daniel, H. (2014). Inhibition of the intestinal sodium-coupled glucose transporter 1 (SGLT1) by extracts and polyphenols from apple reduces postprandial blood glucose levels in mice and humans. *Molecular nutrition & food research, 58*(9), 1795-1808.

Schwingshackl, L., Christoph, M., & Hoffmann, G. (2015). Effects of olive oil on markers of inflammation and endothelial function—a systematic review and meta-analysis. *Nutrients, 7*(9), 7651-7675.

Song, W.-Y., Aihara, Y., Hashimoto, T., Kanazawa, K., & Mizuno, M. (2015). (−)-Epigallocatechin-3-gallate induces secretion of anorexigenic gut hormones. *Journal of clinical biochemistry and nutrition, 57*(2), 164-169.

Sun, E. W., de Fontgalland, D., Rabbitt, P., Hollington, P., Sposato, L., Due, S. L., Wattchow, D. A., Rayner, C. K., Deane, A. M., & Young, R. L. (2017). Mechanisms controlling glucose-induced GLP-1 secretion in human small intestine. *Diabetes, 66*(8), 2144-2149.

Talhaoui, N., Gómez-Caravaca, A. M., León, L., De la Rosa, R., Fernández-Gutiérrez, A., & Segura-Carretero, A. (2016). From olive fruits to olive oil: Phenolic compound transfer in six different olive cultivars grown under the same agronomical conditions. *International journal of molecular sciences, 17*(3), 337.

Valli, V., Danesi, F., Gianotti, A., Di Nunzio, M., Saa, D. L. T., & Bordoni, A. (2016). Antioxidative and anti-inflammatory effect of in vitro digested cookies baked using different types of flours and fermentation methods. *Food Research International, 88*, 256-262.

Valli, V., Taccari, A., Di Nunzio, M., Danesi, F., & Bordoni, A. (2018). Health benefits of ancient grains. Comparison among bread made with ancient, heritage and modern grain flours in human cultured cells. *Food Research International, 107*, 206-215.

Wren, A., & Bloom, S. (2007). Gut hormones and appetite control. *Gastroenterology, 132*(6), 2116-2130.

577
578
579
580
581
582
583
584
3
4
5
8
9
10
11
12
13
14
15
16
17
18
19
20
21
22
23
24
25
26
27
28
29
30
31
32
33
34
35
36
37
38
39
40
41
42
43
44
45
46
47
48
49
50
51
52
53
54
55
56
57
58
59
60
61
62
63
64
65

585 **Table 1**

586 Nutritional composition of DOP.

Humidity (g/100g)	3,53
Protein (g/100g)	12,15
Fat (g/100g)	3,7
Total Fiber (g/100g)	30,8
Insoluble Fiber (g/100g)	24,8
Soluble Fiber (g/100g)	6,06
Ash (g/100g)	10
Carbohydrates (g/100g)	40
Sodium (mg/kg)	182
Saturated Fats (%)	19,74
MUFA (%)	52,32
PUFA (%)	27,92
Total ω3 (%)	2,7
Total ω6 (%)	25,17
ω3/ω6	0,11

587

588

Table 2

TAC and TPC of PRE. TAC is expressed as mM trolox equivalent (TE). TPC is expressed as mg gallic acid equivalent (GAE)/mL. Data are mean ± SD of two independent extractions analyzed in triplicate.

TAC (mM TE)	5.72 ± 0.05
TPC (mg GAE/mL)	0.69 ± 0.06

Table 3

List of metabolites whose signals were assigned and integrated into the NMR spectra. In each condition, data are mean ± SD of three samples coming from independent experiments. Statistical analysis was by the one-way ANOVA followed by Tukey HSD multiple comparison Test ($p<0.05$) for post hoc group comparisons. Similar letters indicate no significant difference.

Metabolites	Bins' Integrals (10^{-3})			
	0 µg/mL	50 µg/mL	200 µg/mL	500 µg/mL
UMP	0.62 ± 0.3^{bc}	1.42 ± 0.48^{ab}	1.99 ± 0.37^{a}	0.03 ± 0.40^{c}
Glucose-6-Phospate	1.39 ± 0.42^{bc}	1.23 ± 0.18^{c}	1.75 ± 0.18^{ab}	5.85 ± 0.87^{a}
o-Phosphocholine	5.28 ± 1.03^{ab}	6.27 ± 0.53^{a}	4.68 ± 0.72^{b}	2.81 ± 0.40^{c}
Lactate	3.72 ± 1.36^{a}	3.74 ± 1.08^{a}	3.70 ± 0.89^{ab}	1.37 ± 0.10^{b}
UDP-N-Acetylglucosamine	2.42 ± 0.18^{c}	2.29 ± 0.18^{c}	3.35 ± 0.64^{b}	8.48 ± 0.82^{a}
Glucose	5.27 ± 0.57^{b}	5.27 ± 0.12^{b}	5.93 ± 0.82^{b}	10.56 ± 1.48^{a}
Ethanol	5.21 ± 1.23^{b}	4.99 ± 1.83^{b}	6.73 ± 3.42^{a}	12.5 ± 2.48^{a}
myo-Inositol	4.16 ± 0.42^{b}	4 ± 0.87^{b}	4.94 ± 1.21^{ab}	8.33 ± 1.04^{a}
Glycine	20.03 ± 6.27^{a}	12.6 ± 2.73^{a}	12.5 ± 2.09^{a}	6.00 ± 1.35^{b}
Taurine	4.42 ± 1.34^{a}	4.67 ± 1.15^{a}	3.88 ± 0.38^{ab}	2.11 ± 0.02^{b}
Pyruvate	4.78 ± 1.17^{a}	4.02 ± 0.4^{a}	3.06 ± 0.41^{b}	1.18 ± 0.29^{b}
Alanine	8.37 ± 0.34^{a}	7.25 ± 0.24^{a}	5.04 ± 0.91^{ab}	1.33 ± 0.45^{b}
Leucine	4.66 ± 0.53^{a}	3.73 ± 0.62^{b}	3.48 ± 0.23^{b}	2.12 ± 0.67^{c}
Isoleucine	4.28 ± 0.6^{a}	4.23 ± 0.59^{b}	4.31 ± 0.34^{b}	1.72 ± 0.29^{c}

Table 4

Cytokine secretion in basal and inflamed condition. Data are expressed as pg/mL and are mean ± SD of four samples in each condition from two independent experiments. Statistical analysis was by the one way ANOVA (IL-1α in basal and stressed condition: $p<0.05$; IL-8 in basal and stressed condition $p<0.001$; IL-10 in stressed condition $p<0.01$) using Dunnett's as post-test to compare supplemented cells to corresponding controls (* $p<0.05$; ** $p<0.01$; *** $p<0.001$). The limit of detection were 4.75 fg/ml, 0.177 pg/ml, 3 fg/mL, 40.5 fg/ml, 9.72 fg/ml, 30.1 fg/ml, 59 fg/ml, 0.25 pg/ml, 0.74 pg/ml for IFNγ, IL-1α, IL-1β, IL-2, IL-4, IL-6, IL-10, IL-12p70, and TNFα respectively.

Polyphenols (µg/mL)	0	50	200	500	0	50	200	500
					IL-1β (10 ng/mL)			
IFNγ	n.d.	0.02±0.03	0.03±0.04	0.02±0.03	0.05±0.01	0.04±0.03	0.08±0.03	0.09±0.03
IL-1α	n.d.	0.75±0.72	0.87±0.58	1.48±0.66**	2.06±0.81	2.2±0.85	3.16±0.61	4.1±1.49*
IL-1β	n.d.	0.03±0.06	0.06±0.1	0.01±0.02	1.21±0.03	0.3±0.0	0.12±0.08	1.13±2.14
IL-2	n.d.	0.05±0.05	0.06±0.04	0.06±0.06	0.11±0.04	0.12±0.04	0.17±0.03	0.2±0.06
IL-4	n.d.	0.03±0.04	0.01±0.02	0.01±0.01	0.09±0.04	0.07±0.04	0.12±0.05	0.17±0.05
IL-6	n.d.	0.03±0.04	0.04±0.03	0.03±0.05	0.16±0.02	0.1±0.05	0.14±0.04	0.16±0.05
IL-8	13.17±4.31	7.97±2.92*	7.84±1.87*	0.11±0.25***	105.2±28.02	21.96±5.25***	9.24±1.02***	0.88±0.4***
IL-10	n.d.	0.05±0.09	0.04±0.06	0.07±0.13	0.17±0.06	0.17±0.11	0.25±0.09	0.37±0.04*
IL-12p70	n.d.	0.3±0.68	0.3±0.66	0.49±1.1	1.64±0.74	1.19±0.99	2.71±1.08	3.29±0.86
TNFα	n.d.	0.84±1.02	n.d.	n.d.	1.96±0.47	1.58±0.57	2.51±0.68	2.88±0.48

Figure Captions

Fig. 1. Phenolic profile and concentration.

Phenols concentration is expressed as µg/mL. Data are mean ± SD of three determination. A representative chromatogram is reported, and peak assignment is given in the table. DAFOA[a], DiAldehydic Form of Oleuropein Aglycone; AFOA[b], Aldehydic Form of Oleuropein Aglycone (5S,8R,9S).

Fig. 2. Cell count and cell viability by TB and by MTT, Alamar Blue assay, and LDH release.

Cell count and cell viability by TB (panel A) are expressed as number of cells per well. Cell viability by MTT and Alamar Blue (panel B) are expressed as percentage of control cells (assigned as 100%). LDH (panel B) is expressed as $mU/mL/10^6$ cells. In each condition, data are mean ± SD of six samples obtained from two independent experiments. Statistical analysis was by the one way ANOVA ($p<0.001$) using Dunnett's as post-test to compare supplemented cells to control ones (* $p<0.05$; ** $p<0.01$; *** $p<0.001$).

Fig. 3. 600.13 MHz ^{1}H NMR spectrum of 4 cell lysate at pH 7.33 and at different concentration of PRE (0, 50, 200 and 500 µg/mL).

Panel A: upfield and midfield region (0.5:4.60). Panel B: downfield region (4.60:9.00). **1**-Leucine (d: 0.946), **2**-Valine (d: 0.978, d: 1.031), **3**-Isoleucine (t: 0.926, d: 0.978), **4**-Ethanol (t: 1.174, q: 3.651), **5**-Lactate (d: 1.318, q: 4.106), **6**-Alanine (d: 1.469), **7a**-Putrescine (m: 1.754, m: 3.048) only in C200 and **7b**-2-Oxoglutarate (t: 2.429; t: 2.996) only in C500, **8**-Acetate (s: 1.909), **9**-Glutamate (m: 2.0403, m: 2.118, m: 2.328), **10**-UDP-N-Acetylglucosamine (s: 2.0716, m: 5.505, m: 5.971, d: 7.9387), **11**-1,3-Dihydroxyacetone (s: 4.413), **12**-Choline (s: 3.192), **13**-Creatine (s: 3.028), **14**-Creatine phosphate (s: 3.032), **15**-O-Phosphocoline (s: 3.209, m: 3.581, m: 4.155), **16**-Taurine (t: 3.249, t: 3.415), **17**-Myo-Inositol (dd: 3.528, t: 3.615, t: 4.056), **18**-Threonine (d: 1.378, d: 3.578, m: 4.249), **19**-Glycine (s: 3.552), **20**-Pyruvate (s: 2.358), **21**-Glucose-1-phosphate (t: 3.391, q: 5.445), **22**-Uridine (m: 5.903, d: 7.860), **23**-Fumarate (s: 6.509), **24**-Tyrosine (d: 6.889, d: 7.184), **25**-Phenyalanine (d: 7.321, t: 7.369, t: 7421), **26**-Nicotinurate (q: 7.590, m: 8.244, dd: 8.703, d: 8.931)**, 27**-Hypoxanthine (s: 8.181, s: 8.201), **28**-Inosine (s: 8.224, s: 8.333), **29**-Formate (s: 8.444), **30**-Glucose-6-phosphate (d: 5.229, m: 3.494), **31**-sn-Glycero-3-phosphocholine (s: 3.218, m: 4.313), **32**-UMP (d: 8.083, m: 5.938). Abbreviations for multiplicities are: s = singlet, dd = doublet of doublets, d = doublet, t = triplet and m = multiplet (denotes complex pattern).

23

Fig. 4. PCA scores plot of the ^{1}H-NMR spectrum for all samples performed on selected significant bins.

(A); PCA plot on the whole spectra dataset. (B); PCA plot on selected bins. The grey scaled arrow from high to low PC1's values stands for the increasing concentration of a pattern of metabolites due to the different PRE concentration. (C) Loadings barplot for the first principal component on the 93 selected bins. 1-2: "UMP"; 3-5: "Glu-6-Phospate"; 6-8: "sn-3-GlyPhoCholine"; 9-11: "o-PhospCholine"; 12-14: "Lactate"; 15-26: "Patterns of signals from different metabolites"; 27-29: "UDP-N-Acetylglucosamine"; 30-38: "Glucose"; 39-41: "Ethanol"; 42: "Myo-Inositol"; 43-45: "o-PhospCholine"; 46: "Glycine"; 47-48: "Myo-Inositol"; 49-60: "Glucose"; 61-63: "Taurine"; 64: "Glucose"; 65-67: "o-PhospCholine"; 68: "Choline"; 69: "Pyruvate"; 70-71: "Not Assigned"; 72-74: "Alanine"; 75:78: "Lactate"; 79-81: "Not Assigned", 82-84: "Ethanol"; 85-86: "Leucine"; 87-88: "Isoleucine"; 89-93: "Not Assigned".

Fig. 5. IL-8 secretion in basal (A) and inflammatory condition (B).

IL-8 is expressed as pg/mL. In each condition data are mean $\pm$ SD of nine samples obtained from three independent experiments. Statistical analysis was by the one way ANOVA ($p<0.001$) using Dunnett's as post-test to compare supplemented cells to corresponding controls (*** $p<0.001$).

Figure 1

| #	Compounds	Mass data ESI⁻	μg/ml
1	Quinic acid	191 [M-H]⁻, 111	73.7 ± 10.1
2	Hydroxytyrosol 4-β-D-glucoside	315 [M-H]⁻, 153	37.3 ± 9.3
3	1-β-D-glucopyranosyl acyclodihydroelenolic acid / Hydroxytyrosol	407 [M-H]⁻	111.5 ± 6.9
4	Tyrosol	137 [M-H]⁻	11.8 ± 0.1
5	*p*-coumaric acid	153 [M-H]⁻, 123	6.5 ± 0.2
6	Caffeic acid	179 [M-H]⁻, 135	7.4 ± 0.2
7	DAFOA [a] (Decardoxymethylated)	377 [M-H]⁻, 307	21.1 ± 2.3
8	Hydroxylariciresinolglucoside	537 [M-H]⁻	5.2 ± 0.1
9	β-Hydroxyverbascoside diastereoisomers	639 [M-H]⁻	114.9 ± 6.7
10	β-Hydroxyverbascoside diastereoisomers	639 [M-H]⁻	125.4 ± 7.2
11	Rutin	609 [M-H]⁻	12.0 ± 1.3
12	Verbascoside	623 [M-H]⁻	57.8 ± 4.4
13	Dihydro-oleuropein	543 [M-H]⁻	14.0 ± 1.7
14	Isoverbascoside	623 [M-H]⁻	19.4 ± 1.4
15	Deacetoxy oleuropein aglycone	319 [M-H]⁻	67.3 ± 4.0
16	Oxidized product of DAFOA [a]	335 [M-H]⁻	32.7 ± 0.6
17	Hydro-oleuropein	539 [M-H]⁻	11.7 ± 0.1
18	AFOA [b]	377 [M-H]⁻	10.3 ± 1.4
19	AFOA [b]	377 [M-H]⁻	9.8 ± 0.8
	Total phenolic contents		749.2 ± 17.6
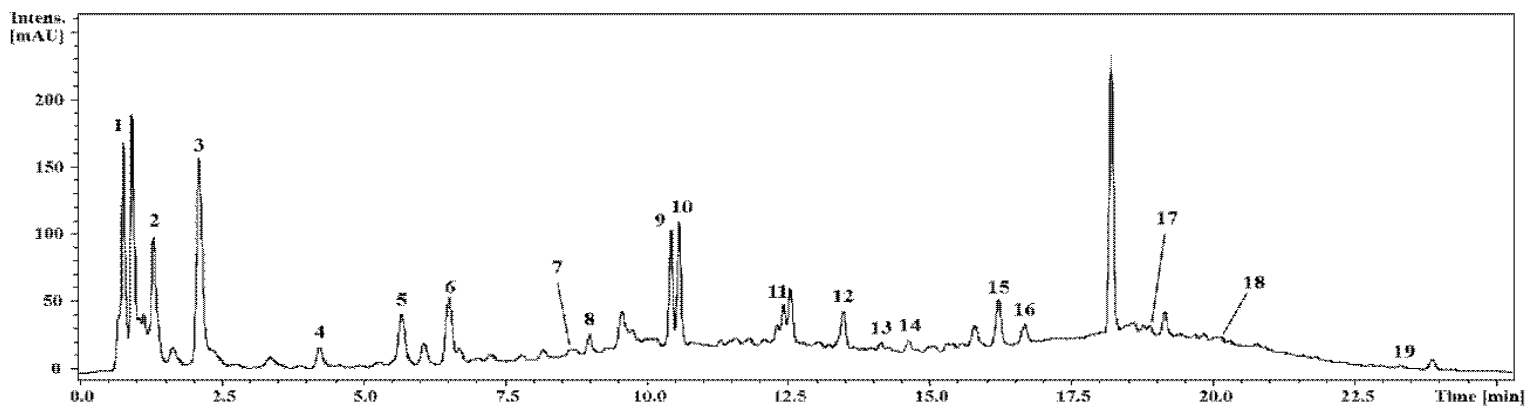
Figure 2

Figure 3

Figure 4

A

B

C

PRE Concentration (μg phenol/mL)
☐ 0 ● 50 ▲ 200 ◆ 500

5.980 ppm   0.876 ppm

Figure 5

A

B
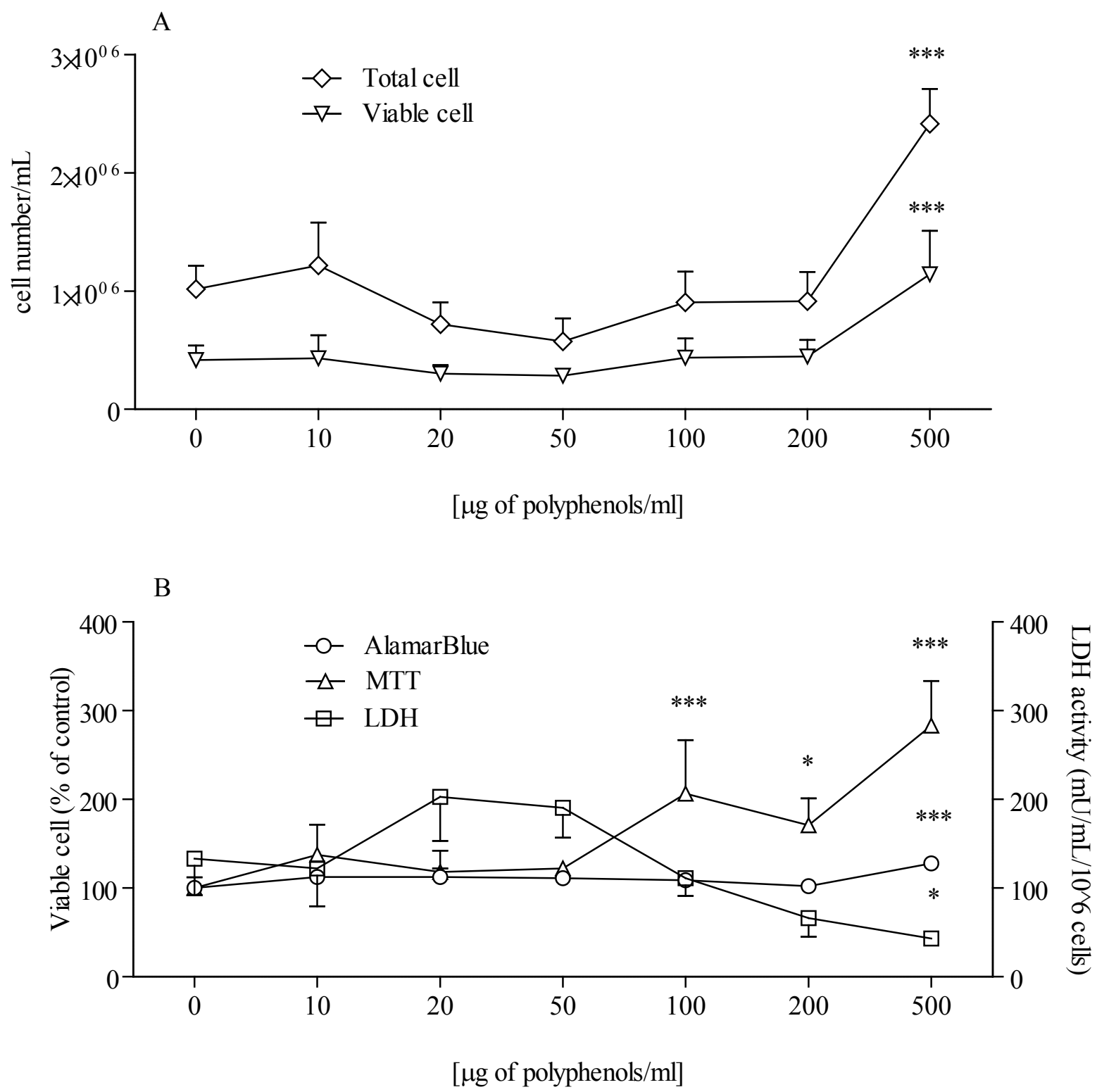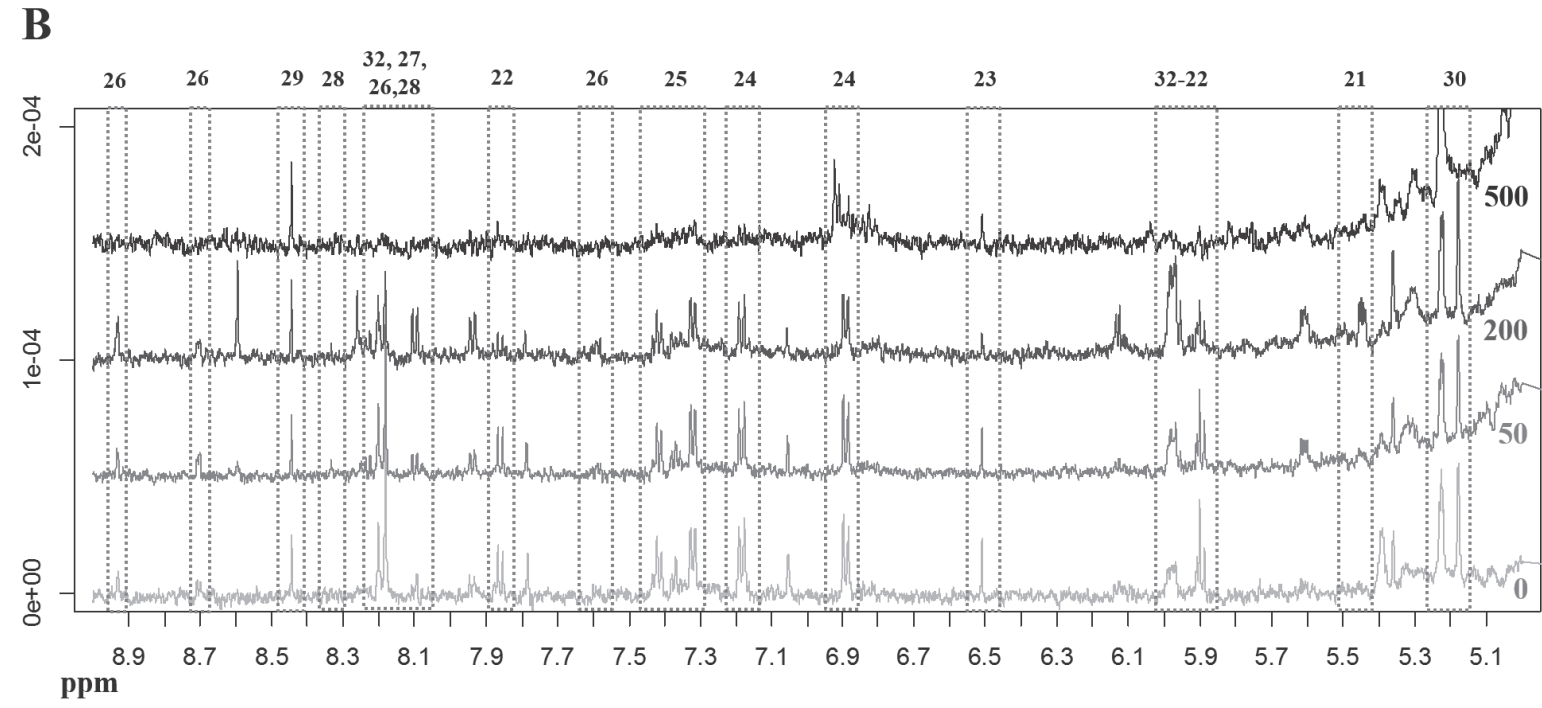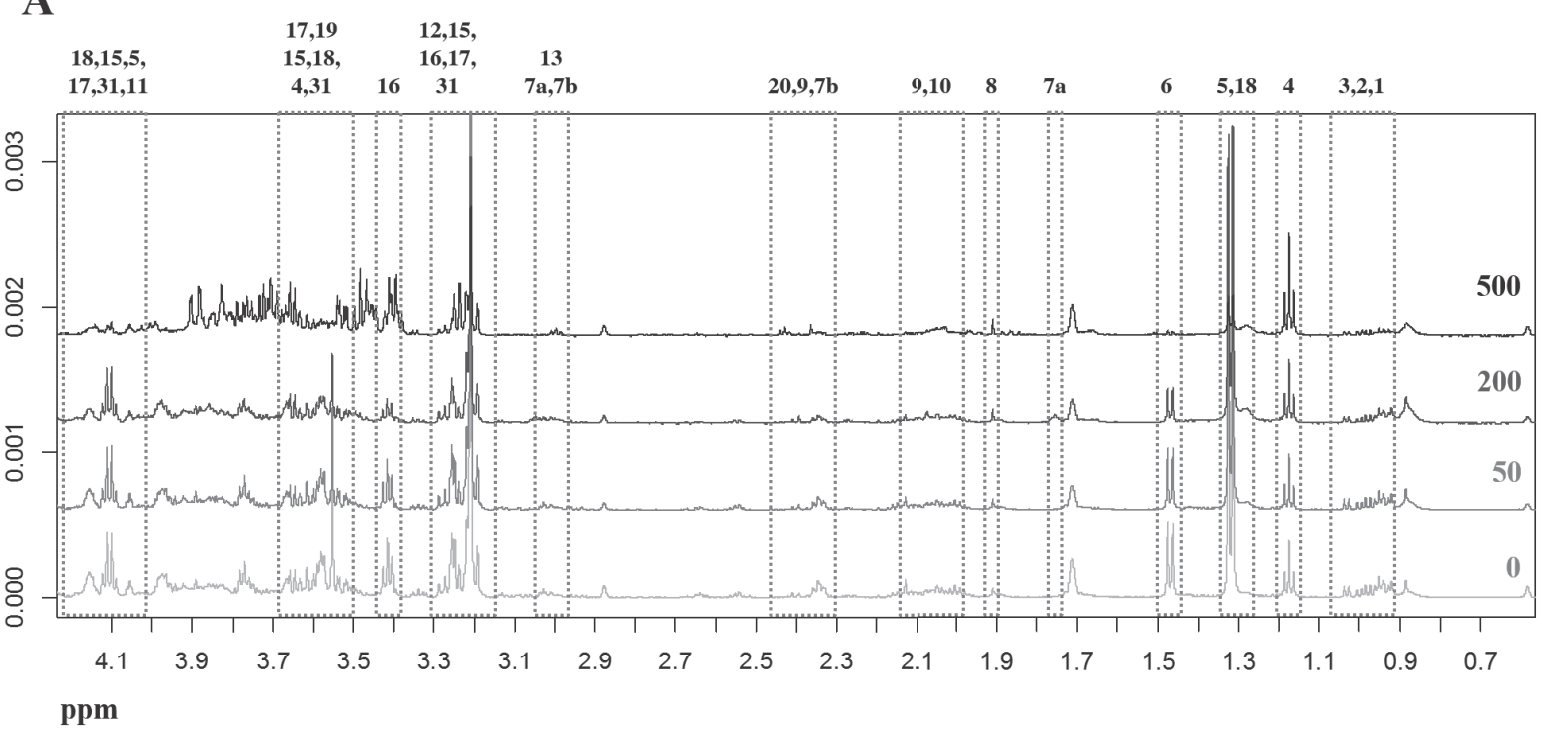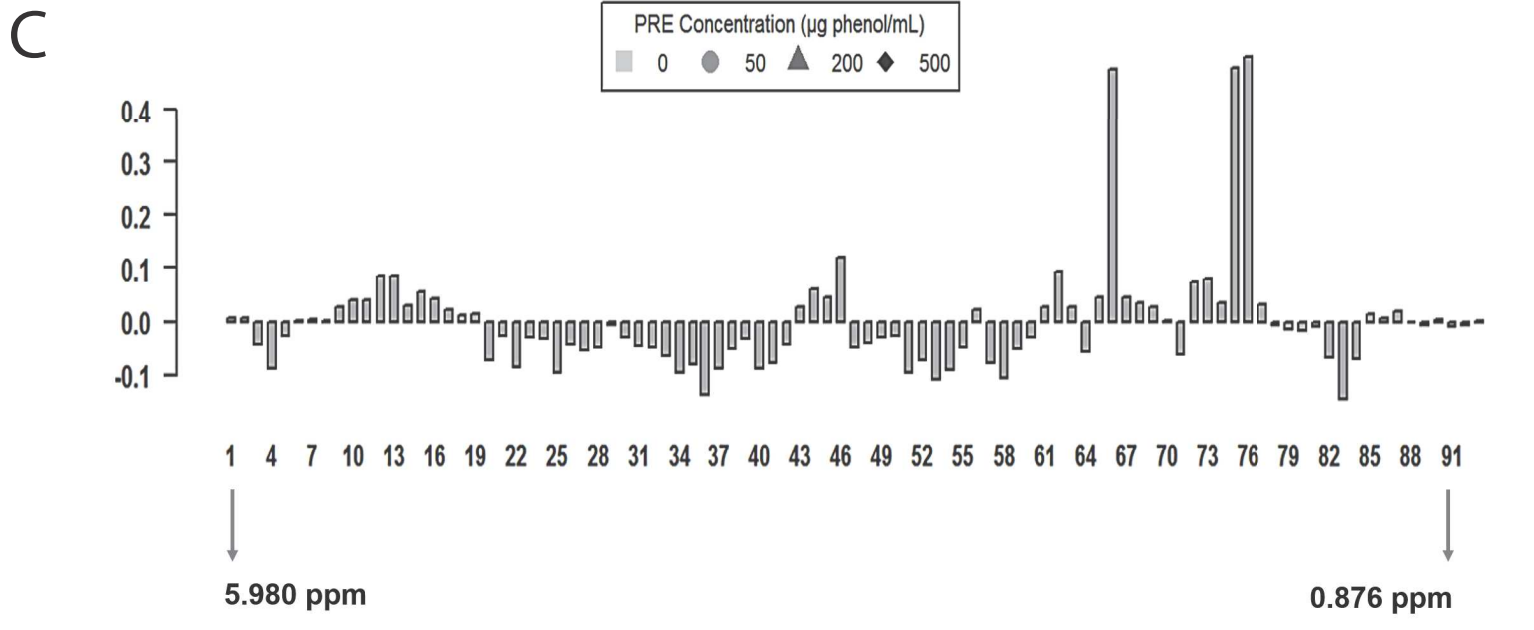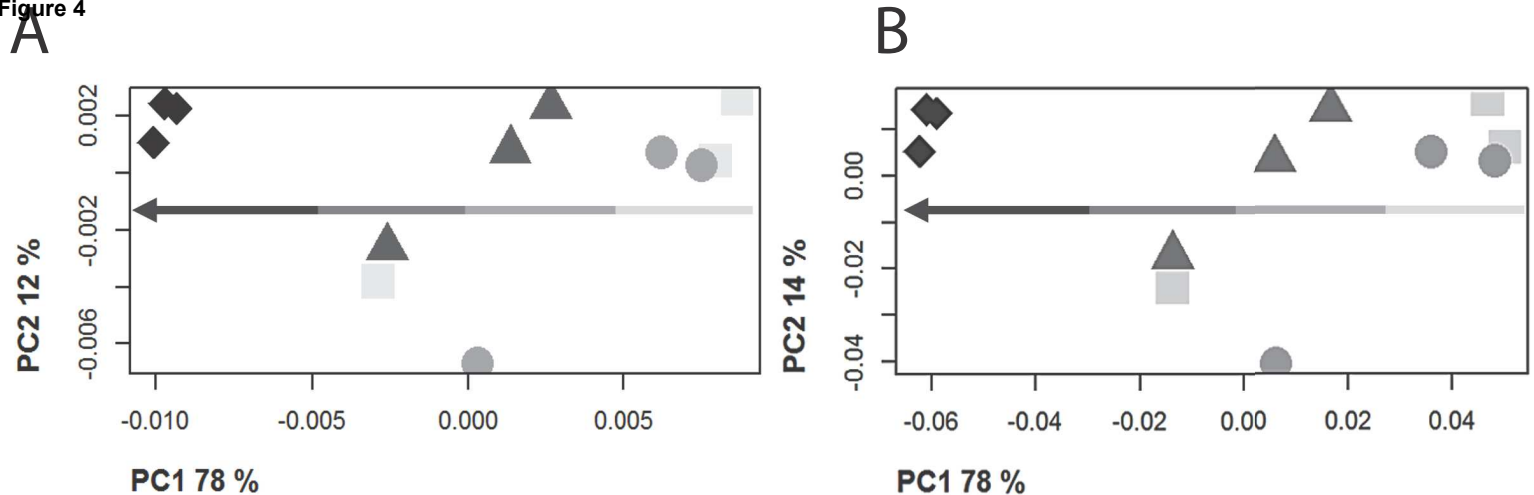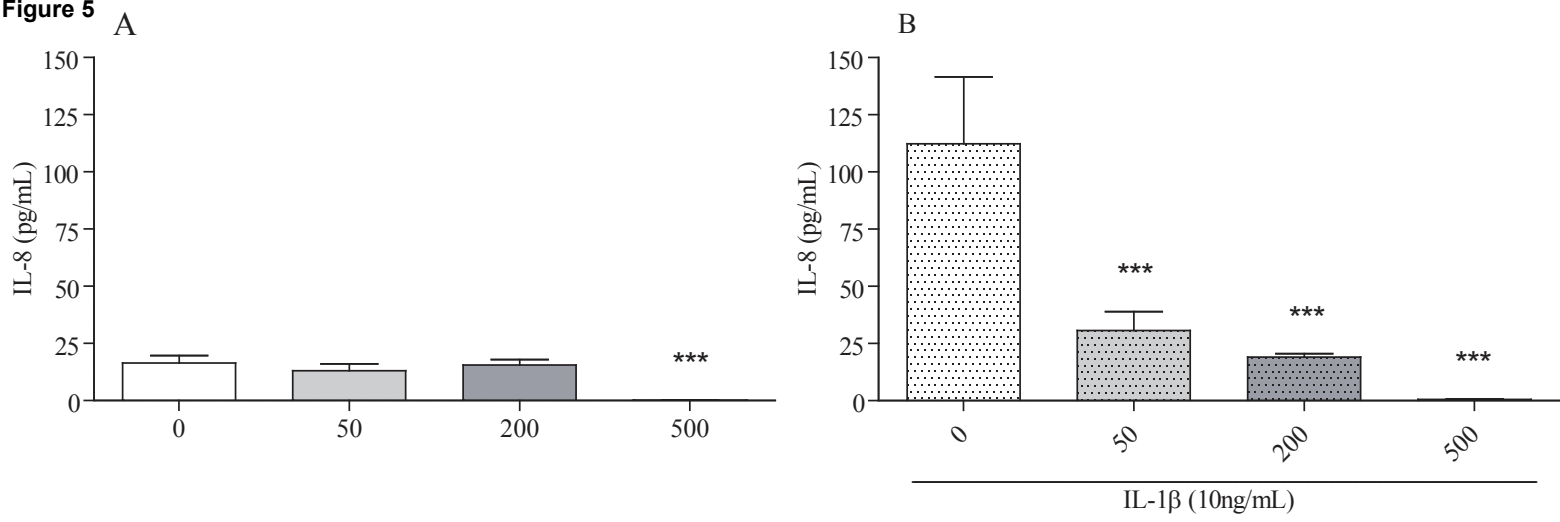
*Graphical Abstract

Olive oil by-products — **HPLC Phenol Quantification** — **Intestinal cells *In vitro* model** — **NMR Nutri-Metabolomics**

Olives — Phenol-rich ingredient — Olive Pomace

Phenol-rich extract (PRE)

Caco-2 Cells — Caco-2 Cells — Phenol-rich extract (PRE) Supplementation

Anti-inflammatory effect

↑ Glucose

OLIVE OIL INDUSTRY BY-PRODUCTS. EFFECTS OF A POLYPHENOL-RICH EXTRACT ON THE METABOLOME AND RESPONSE TO INFLAMMATION IN CULTURED INTESTINAL CELL